Research Square

Preprints are preliminary reports that have not undergone peer review.
They should not be considered conclusive, used to inform clinical practice,
or referenced by the media as validated information.

# Mechanical Force Modulates Periodontal Ligament Stem Cell Characteristics During Bone Remodeling via TRPV4

**Shan-Shan Jin**
Peking University School of Stomatology
**Dan-Qing He**
Peking University School of Stomatology
**Yu Wang**
Peking University School of Stomatology
**Ting Zhang**
Peking University School of Stomatology
**Hua-Jie Yu**
Peking University School of Stomatology
**Zi-Xin Li**
Peking University School of Stomatology
**Li-Sha Zhu**
Peking University School of Stomatology
**Yan-Heng Zhou**
Peking University School of Stomatology
**Yan Liu** ( orthoyan@bjmu.edu.cn )
Peking University School of Stomatology https://orcid.org/0000-0002-8193-6729

**Research**

**Keywords:** Mechanical force, periodontal ligament stem cells, cell functions, TRPV4, bone remodeling

**Posted Date:** June 26th, 2020

**DOI:** https://doi.org/10.21203/rs.3.rs-36699/v1

**License:** This work is licensed under a Creative Commons Attribution 4.0 International License.
Read Full License

# Abstract

**Background:** Mechanical force plays an important role in modulating stem cell fate and behaviors, thereby guiding tissue development, homeostasis, and regeneration. However, how periodontal ligament stem cells (PDLSCs) perceive the mechanical stimulus and transfer it into biological signals, and thereby promote alveolar bone remodeling, is unclear.

**Methods:** An animal model of mechanical force-induced tooth movement and a compressive force stimulus *in vitro* were used in the present study. After force application for 3 and 7 days, the tooth movement distance, the number of mesenchymal stem cells and osteoclasts, and the expression of the proinflammatory cytokines were detected in periodontal tissues. Then, PDLSCs with or without force loading were isolated *ex vivo* and their stem cell characteristics including clonogenicity, proliferation, multipotent differentiation, and immunoregulatory properties were evaluated. Under the compressive force stimulus *in vitro*, the effects of the ERK signaling pathway on the PDLSC characteristics were evaluated by Western blotting.

**Results:** Mechanical force *in vivo* induced PDLSC proliferation, which was accompanied with inflammatory cytokine accumulation, osteoclast differentiation and TRPV4 activation; mechanical force changed the stem cell characteristics of load-induced PDLSCs isolated *ex vivo*, showing greater clonogenicity and proliferation, reduced differentiation ability, improved induction of macrophage migration, osteoclast differentiation, and proinflammatory factor expression. The biological changes induced by mechanical force could be partially suppressed by a small-molecule antagonist of TRPV4. Mechanistically, the potential communication between mechanical force and biological response through the ERK signaling was activated by TRPV4.

**Conclusions:** Taken together, we show here that the activation of TRPV4 in PDLSCs under mechanical force contributes to the changes in their stem cell characteristics including clonogenicity, proliferation, multipotent differentiation, and immunoregulation and modulates bone remodeling during tooth movement.


# Background

Pluripotent mesenchymal stem cells (MSCs) contribute to multiple physiological and pathological processes, including development, inflammation, disease recovery, tissue remodeling, and regeneration [1–3]. Mechanical force plays an important role in modulating MSC fate and behaviors, and thereby guiding development, homeostasis, and regeneration [4]. *In vivo* experiments have shown that mechanical force influences the functions of MSCs during force-induced bone remodeling or cardiac injury remodeling [5, 6]. Furthermore, mechanical stimuli—including pressure, shear stress, and stretch—applied *in vitro* has been shown to modulate MSC differentiation by mobilizing second messengers, ion channels, and cytoskeleton or membrane proteins such as integrins [7].

The periodontal ligament (PDL) is a soft connective tissue embedded between two different hard tissues, the root of tooth and the alveolar bone, that stabilizes teeth and relieves the pressure caused by masticatory force [8]. It plays an important role in maintaining tissue homeostasis and provides a microenvironment for inflammatory reactions and bone remodeling under mechanical stimulation. Mechanical force-induced tooth movement through the alveolar bone relies on the PDL, and is a unique local aseptic inflammation-associated process of bone remodeling [9]. Periodontal ligament stem cells (PDLSCs), as the main MSCs in the PDL microenvironment [10], exhibit clonogenicity, proliferation, multipotent differentiation, and immunoregulatory properties. They respond to mechanical force by producing high levels of inflammatory cytokines and chemokines, playing an important role in alveolar bone remodeling [11–13]. However, how PDLSCs perceive the mechanical stimulus and transfer it into biological signals, thereby contributing to alveolar bone remodeling, needs further investigation.

Mechanosensitive channels are sensors of mechanical stimulation in various cell types [14]. The transient receptor potential (TRP) calcium channel is involved in the sensation of various stimuli in various tissues and cell types [15]. TRP subfamily V member 4 (TRPV4) regulates mechanosensation, inflammation, and energy homeostasis. Moreover, mutations in TRPV4 are associated with inherited disorders of bone metabolism [16]. MSCs isolated from TRPV4 knockout mice demonstrate impaired osteogenic potential [17]. Therefore, we hypothesized that the stem cell characteristics of PDLSCs are influenced by the activation of TRPV4 under mechanical stimuli, which promote alveolar bone remodeling and tooth movement. Using an animal model of mechanical force-induced tooth movement and a compressive force stimulus *in vitro*, we herein evaluated the biological changes of PDLSCs, including their clonogenicity, proliferation, multipotent differentiation, and immunoregulatory properties, under mechanical stimuli. Universal upregulation of TRPV4 in PDLSCs as well as the underlying molecular mechanism under mechanical force are demonstrated. These results together pinpoint the importance of mechanical force-induced TRPV4 in regulating the stem cell characteristics of PDLSCs and mediating bone remodeling.

## Methods

# An Experimental Animal Model of Mechanical Loading

Male Sprague–Dawley rats 6–8 weeks of age (Weitong Lihua Experimental Animal Center, Beijing, China) were used in this study. The animal experimental protocols were approved by the Institutional Animal Care and Use Committee of Peking University (LA2013-92). To establish an experimental animal model of mechanical loading, nickel-titanium coil springs (0.2 mm thickness, 1 mm diameter, 4 mm length; Smart Technology, Beijing, China) were ligated between the right maxillary first molar and the incisors (Fig. S1). Each coil spring can provide a constant force of ~ 0.6 N to move teeth [11, 18, 19]. The contralateral first molar served as the control. After 3 and 7 days of treatment (F 3d, F 7d), the rats (n = 6) were sacrificed by overdose of pentobarbital sodium, and the maxillae were harvested, fixed in 4% paraformaldehyde (PFA), and scanned by Micro-computed tomography (micro-CT, Skyscan1174, Bruker, Belgium) at a resolution of 10 μm. The acquired axial images were imported into a NRecon and CTvox software for 3-D

reconstruction. Another 12 rats on day 7 were sacrificed by excessive anesthesia and the maxillary first molars of both sides were separated for the culture of primary cells. An occlusal view of the maxillae was obtained using a stereomicroscope (SWZ1000, Nikon). The distance of tooth movement induced by the mechanical loading was measured using a modified method described previously [19]. Briefly, the distance between two easily located points (the midpoint of the distal-marginal ridge of the first molar and the midpoint of the mesial-marginal ridge of the second molar) was measured by two trained researchers, who were blinded to the group assignment. The average of two measurements was calculated as the tooth movement distance.

# Hematoxylin and Eosin and Tartrate-Resistant Acid Phosphatase Staining

The fixed maxillae were demineralized in 15% ethylenediaminetetraacetic acid and embedded in paraffin. Consecutive 4-μm-thick transverse sections were obtained from the corresponding group and stained with hematoxylin and eosin (H&E) and tartrate-resistant acid phosphatase (TRAP) staining. TRAP staining was performed using an acid phosphatase kit (387A-1KT; Sigma) according to the manufacturer's instructions. TRAP-positive, multinucleated (> 3 nuclei) cells attached to the alveolar bone surface were counted (n = 5) [20].

# Immunofluorescence Staining

Immunofluorescence staining was performed as described previously [21]. Tissue sections were double-stained with anti-CD146 (1:200, ab-75769, Abcam) and anti-Ki67 (1:200, ab8191; Abcam) or anti-TRPV4 (1:200, ab39260; Abcam) antibodies. Other sections were stained with anti-interleukin (IL)-6 (1:200, ab9324; Abcam) and anti-IL-1β (1:200, ab9722, Abcam) antibodies. Next, the sections were incubated with fluorescein isothiocyanate-conjugated or tetramethylrhodamine isothiocyanate-conjugated secondary antibodies (1:200; Jackson ImmunoResearch Laboratories). Nuclei were counterstained with 4',6-diamidino-2-phenylindole. Confocal microscopic images were processed with LSM 5 Release 4.2 software following acquisition with a laser-scanning microscope (LSM 510; Zeiss).

# Isolation, Culture, and Treatment of PDLSCs

To obtain rat PDLSCs (rPDLSCs) subjected to *in vivo* mechanical loading (F-PDLSCs), periodontal tissues from the rat maxillary force-induced first molar were lightly separated, minced, and digested in a fresh enzyme mixture, comprising 3 mg/mL collagenase type I (Worthington Biochemical) and 4 mg/mL dispase II (Roche Diagnostics) for 60 min at 37 °C. After passing through a 70-μm strainer, single-cell suspensions were cultured in α-modified Eagle's medium supplemented with 15% fetal bovine serum, 2 mM L-glutamine, and 100 U/mL penicillin/streptomycin. rPDLSCs isolated from normal periodontal tissues (N-PDLSCs) in the contralateral first molar served as the control. To remove the nonadherent cells,

the cultures were washed twice with phosphate-buffered saline (PBS). The attached primary cells were cultured for 10 days and then were subcultured. rPDLSCs at passage 2 were used in this study. To inhibit expression of TRPV4 in force-induced rPDLSCs, a pharmacological antagonist (GSK2193874, Selleck) was added to the culture medium with the final concentration of 10 μM.

Human PDLSCs (hPDLSCs) were isolated from extracted teeth and cultured as described previously [10]. Permission to obtain extracted teeth was provided by the Ethics Committee of Peking University (PKUSSIRB-201311103). hPDLSCs isolated from 3 different individuals were pooled together and cells at passages 2–3 were used in this study. Static compressive force was applied to the hPDLSCs as described previously [13]. Briefly, a layer of glass and additional metal balls were placed on a 70–80% confluent cell layer in six-well plates. hPDLSCs were subjected to static compressive forces of 0–1.5 g/cm$^2$ for 12 h.

To inhibit the activation of TRPV4 in hPDLSCs, GSK2193874 (10 μM) was added to the medium for 1 h prior to compressive force stimulation (1.5 g/cm$^2$, 12 h). To activate the TRPV4, hPDLSCs were treated by a pharmacological agonist (GSK1016790A, Selleck) with the final concentration of 10 nM for 1 h. For the control group, dimethyl sulfoxide (DMSO) of the same volume was added.

# Cell Proliferation and Colony Forming Units-fibroblastic Assay

Cell proliferation was monitored using a CCK-8 kit (Sigma) according to the manufacturer's instructions. Rat PDLSCs isolated *ex vivo* were incubated with CCK-8 reagent at 37 °C for 2 h. Next, the absorbance at 450 nm was measured using a microplate reader (Bio-Rad, Japan).

Cells (500 per well) were seeded and incubated in six-well plates for 14 days in growth medium and fixed with 4% PFA (Sigma). Next, 0.1% crystal violet was used to stain the cells. Colonies of more than 50 cells were defined as single colony clusters, and the number of clusters was counted.

# Multipotent Differentiation of PDLSCs *Ex Vivo*

We evaluated the multi-differentiation potential of rPDLSCs isolated *ex vivo* with or without force loading toward osteogenesis and adipogenesis as reported previously [10]. To induce osteogenesis, the medium was changed to osteogenic medium (growth medium with 10 nM dexamethasone, 100 μM ascorbic acid 2-phosphate, and 10 mM β-glycerophosphate). After culture in osteogenic medium for 21 days, the cells were fixed in 4% PFA and stained with 1% Alizarin Red S (Sigma) at room temperature. The Alizarin Red-positive area was measured using ImageJ software and is expressed as the percentage of Alizarin Red-positive area over the total area. For adipogenic induction, cells were cultured in adipogenic medium (growth medium with 500 μM isobutyl-methylxanthine, 60 μM indomethacin, 0.5 μM hydrocortisone, and

10 μM insulin) for 3 weeks. After fixing in 60% isopropanol, the cells were stained with 0.3% Oil Red O (Sigma) and the number of Oil Red O-positive droplet-containing cells was counted.

# Co-culture of PDLSCs and RAW264.7 Macrophages

# Transwell Migration System

To investigate their chemoattractive activity, rPDLSCs isolated *ex vivo* with or without force loading were seeded into six-well plates, and RAW264.7 macrophages were added to the upper chamber of the Transwell migration system at $1 \times 10^5$/well. RAW264.7 macrophages were co-cultured with rPDLSCs isolated *ex vivo* for 24 h, and cells remaining in the upper chamber were gently removed using cotton swabs. After washed twice with PBS, the Transwell chambers were fixed in 4% PFA and stained with 0.1% crystal violet for 15 min. Cells stained by crystal violet on the bottom surface served as the migrated cells and were counted under an inverted microscope.

# Direct Cell-to-Cell Contact System

To investigate their osteoclastogenesis, rPDLSCs isolated *ex vivo* with or without force loading were seeded into 12-well plates at $5 \times 10^3$/well and RAW264.7 macrophages were added at $5 \times 10^5$/well. To induce osteoclast differentiation, soluble receptor activator of nuclear factor-κB ligand (sRANKL) (50 ng/mL) was added to the medium [22]. After co-culturing for 7 days, the cells were fixed and stained with an acid phosphatase kit (387A-1KT; Sigma) for TRAP staining. TRAP-positive, multinucleated (two or more nuclei) osteoclasts were counted in five visual fields per well (n = 3). The final result was the average of three experiments.

# Quantitative Reverse-Transcription Polymerase Chain Reaction

Total RNA was extracted using TRIzol reagent (Invitrogen) according to the manufacturer's instructions. Reverse-transcription and real-time PCR were performed following protocols described in detail previously. The primers (designed using Primer Premier 5.0 software) were as follows: for rat β-actin, sense/antisense: 5'-TGACAGGATGCAGAAGGAGA-3'/5'-TAGAGCCACCAATCCACACA-3'; IL-1β, sense/antisense: 5'-CACCTCTCAAGCAGAGCACAG-3'/5'-GGGTTCCATGGTGAAGTCAAC-3'; tumor necrosis factor (TNF)-α, sense/antisense: 5'-CCAGGTTCTCTTCAAGGGACAA-3'/5'-CTCCTGGTATGAAATGGCAAATC-3'; IL-6, sense/antisense: 5'-CCAAGACCATCCAACTCATCTTG-3'/5'-CACAGTGAGGAATGTCCACAAAC; monocyte chemoattractant protein (MCP)-1, sense/antisense: 5'-CAGCCAGATGCAATCAATGCC-3'/5'-TGGAATCCTGAACCCACTTCT-3'; TPRV1, sense/antisense: 5'-GCCGCTGAACCGACTC-3'/5'-CCCATCTGCTGGAAAC-3'; TPRV2, sense/antisense: 5'-CGCCATTGAGAAGAGGAGTC-3'/5'-GCTTACCACATCCCACTGCT-3'; TPRV3, sense/antisense: 5'-GCGTGGAGGAGTTGGTAGAG-3'/5'-CTCTGTGTACTCGGCGTTGA-3'; and TPRV4, sense/antisense: 5'-

CAGGTGGGGAGGCTTTT-3'/5'-GCGGCTGCTTCTCTATG-3'. For human GAPDH, sense/antisense: 5'-ATGGGGAAGGTGAAGGTCG-3'/5'- GGGGTCATTGATGGCAACAATA; TNF-α, sense/antisense: 5'-CCTCTCTCTAATCAGCCCTCTG-3'/5'- GAGGACCTGGGAGTAGATGAG-3'; IL-6, sense/antisense: 5'-CGGTCCAGTTGCCTTCT-3'/5'- GCCAGTGCCTCTTTGCT; The efficiency of the newly designed primers was confirmed by sequencing the products of conventional PCR.

# Western Blot Analysis

Cells were lysed with RIPA buffer mixed with protease and phosphatase inhibitor cocktail (Thermo Fisher Scientific, USA). Total protein (25 μg) was separated by 10% SDS-polyacrylamide gel and then transferred onto a polyvinylidene difluoride (PVDF) membrane (Millipore, USA). After being blocked in 5% nonfat milk in Tris-buffered saline containing 0.1% Tween-20 for 1 h at room temperature, the membranes were incubated overnight at 4 °C with primary antibodies as following: anti-TRPV4 (ab39260; Abcam), anti-Ki67 (ab8191; Abcam), anti-IL-6 (ab9324; Abcam), anti-RANKL (ab45039, Abcam), anti-osteoprotegerin (OPG) (ab11994, Abcam), anti-phospho-p44/42 MAPK (ERK1/2) (Thr202/Tyr204) (4370, Cell Signaling Technology), anti-p44/42 MAPK (ERK1/2) (4695, Cell Signaling Technology), and anti-glyceraldehyde-3-phosphate dehydrogenase (GAPDH) (3683S, Cell Signaling Technology). Then the membranes were incubated with a horseradish peroxidase-conjugated mouse or rabbit IgG (1:5000; Zhongshanjinqiao, China), and protein bands were detected by enhanced with a SuperSignal West Pico Chemiluminescent Substrate (Thermo Fisher Scientific, USA). The relative density of three comparable results was measured using ImageJ software. Each experiment was repeated three times.

# Statistical Analysis

Statistical Package for the Social Sciences 19.0 software was used to perform statistical analysis. Data were presented as means ± standard deviation (SD). The normal distribution of the raw data were confirmed by a one-sample Kolmogorov-Smirnov test, and assessed for significance by two-tailed independent Student's *t*-test or one-way analysis of variance (ANOVA). Tukey's multiple-comparison test was used for the *post-hoc* comparison of ANOVA. Differences with $P < 0.05$ were considered statistically significant.

# Results

### Mechanical Force Induces the Proliferation of PDLSCs and the Expression of Inflammatory Factors during Bone Remodeling and Tooth Movement

The experimental animal model of mechanical loading was fit for purpose, as evidenced by tooth movement of 240.4 ± 40.9 μm on day 3 and 369.7 ± 30.1 μm on day 7 (Fig. 1A). Double immunostaining showed that most Ki67 expression (indicating cell proliferation) colocalized with CD146, a marker of MSCs, in periodontal tissues. After force application for 3 days, the proportion of $CD146^+$ $Ki67^+$ PDLSCs increased to 5.1 ± 1.9% and reached 10.4 ± 2.8% after 7 days compared with the control group (1.9 ±

0.7%), indicating that the proliferation ability of PDLSCs was enhanced after mechanical force stimulation (Fig. 1B). TRAP-positive osteoclasts accumulated in the periodontal tissues, near the alveolar bone, during mechanical loading (Fig. 1C). Moreover, the expression of the proinflammatory cytokines IL-6 and IL-1β increased on the compression side of periodontal tissues after force application (Fig. 1D). Therefore, mechanical force induces PDLSC proliferation *in vivo*, which might be associated with the accumulation of proinflammatory factors and osteoclast differentiation around the periodontal tissues.

**Mechanical Force Changes the MSC Characteristics of rPDLSCs** Ex Vivo

Although PDLSCs, a type of MSCs, have been reported to have self-renewal and multidirectional differentiation potential, their detailed characteristics under mechanical stimuli during bone remodeling remain to be elucidated. Herein, rPDLSCs with or without mechanical loading were isolated *ex vivo* and a variety of experimental techniques were applied for their characterization.

CCK-8 assays showed that proliferation of the force-induced rPDLSCs (F-PDLSCs) was greater than that of normal PDLSCs (N-PDLSCs), which is consistent with the phenomenon *in vivo* (Fig. 2A). Both cell types proliferated slowly from 0 to 3 days. However, from 3 to 7 days, the F-PDLSCs grew more rapidly than the N-PDLSCs. Additionally, the F-PDLSCs showed stronger clone formation ability compared with the N-PDLSCs (Fig. 2B). To evaluate their multi-differentiation ability, cell populations at passage 2 were supplemented with osteoinductive and adipoinductive medium. After 3 weeks of osteogenic induction, the N-PDLSCs produced dramatically more mineralized extracellular matrix (stained with Alizarin Red S) than the F-PDLSCs (Fig. 2C). Moreover, the F-PDLSCs suffered observable impairment of adipogenic differentiation, as shown by decreased accumulation of lipid-rich vacuoles. Quantitative analysis showed that the number of lipid-specific Oil Red O-positive cells in the F-PDLSCs was less than that in the N-PDLSCs (Fig. 2D). These data suggest that rPDLSCs isolated *ex vivo* showed greater proliferation and reduced differentiation ability following mechanical stimulation *in vivo*.

To evaluate the immunomodulatory function of the rPDLSCs, we performed a Transwell migration assay with rPDLSCs isolated *ex vivo* with or without mechanical loading and RAW264.7 macrophages. We found that conditioned medium from the F-PDLSCs promoted the migration of macrophages compared with the N-PDLSCs group (Fig. 2E). We further assessed osteoclast differentiation of F-PDLSCs using a cell-to-cell contact co-culture system with rPDLSCs and RAW264.7 macrophages. TRAP staining showed that the F-PDLSCs *ex vivo* enhanced osteoclast differentiation compared with the N-PDLSCs group (Fig. 2F). In addition, the expression of proinflammatory factors in the PDLSCs isolated *ex vivo* was evaluated. The mRNA levels of IL-1β, TNF-α, IL-6, and MCP-1 were increased in the F-PDLSCs isolated *ex vivo*. The IL-6 protein level was also increased in the F-PDLSCs isolated *ex vivo* (Fig. 2H). Meanwhile, the Ki67 protein level was upregulated after mechanical loading, which further confirmed the result of CCK-8 assay. These results collectively suggest improved induction of macrophage migration, osteoclast differentiation, and proinflammatory factor expression in F-PDLSCs isolated *ex vivo*. Therefore, mechanical stimuli *ex vivo* might alter the MSC characteristics of rPDLSCs, which may contribute to bone remodeling and tooth movement after mechanical force stimulation.

### TRPV4 Channels Are Activated in the Force-induced rPDLSCs Ex Vivo

We next determined how mechanical force was perceived by rPDLSCs and translated into biological signals. Previous studies have demonstrated that TRPV channels are sensitive to microenvironment temperature and mechanical and chemical stimuli [23, 24]. We therefore assayed the mRNA levels of TRPV channels in rPDLSCs. mRNAs of TRPV1–4 were detected in rPDLSCs, while that of TRPV4 was increased in the F-PDLSCs *ex vivo* (Fig. 3A). The TRPV4 protein level in the F-PDLSCs *ex vivo* was about fourfold that in the normal PDLSCs, consistent with the mRNA level (Fig. 3B). To confirm the increased TRPV4 expression after mechanical loading *in vivo*, double immunostaining of TRPV4 and CD146 was performed during mechanical force-mediated tooth movement. After force application, the proportion of $CD146^{+}TRPV4^{+}$ PDLSCs increased to 3.9 ± 0.9% at 3 days and 7.3 ± 1.3% at 7 days compared with the control group (Fig. 3C). These results suggested that TRPV4, as a means of sensing mechanical force, was expressed in PDLSCs after mechanical force stimulation, which may link the transduction of mechanical stimuli with the subsequent biological responses.

### Inhibition of TRPV4 Represses the Biological Characteristics of Force-induced PDLSCs Ex Vivo

Because TRPV4 plays a role in modulating PDLSC function under mechanical force, a small-molecule antagonist, GSK2193874 (hereafter GSK219), was applied to functionally confirm the impact of TRPV4 on the F-PDLSCs *ex vivo*. CCK-8 assays showed that the enhanced proliferation rate of F-PDLSCs *ex vivo* was inhibited by the TRPV4 antagonist GSK219 at 10 μM (Fig. 4A). The clone formation ability of the F-PDLSCs *ex vivo* was also impaired by GSK219 treatment (Fig. 4B). In addition, TRAP staining results showed a significant decline in $TRAP^{+}$ osteoclast differentiation in co-culture of F-PDLSCs *ex vivo* and monocytes following treatment with GSK219 (Fig. 4C). Immunofluorescence staining showed that IL-6 expression in the force-induced PDLSCs *ex vivo* was suppressed by GSK219 treatment (Fig. 4D). Furthermore, the mRNA levels of IL-1β, TNF-α, IL-6, and MCP-1 were decreased in the force-induced PDLSCs *ex vivo* after GSK219 treatment (Fig. 4E). These results collectively suggested a role for force-induced TRPV4 in changes in the proliferative capacity, colony-forming ability, osteoclastic differentiation, and expression of inflammation-related genes in F-PDLSCs.

### Modulation of the NF-κB Ligand/Osteoprotegerin Ratio by TRPV4 in hPDLSCs under Mechanical Force In Vitro

Because TRPV4 expression was enhanced during bone remodeling and tooth movement and modulated the biological properties of force-induced PDLSCs, we evaluated the mechanism by which TRPV4 expression in PDLSCs regulated osteoclastogenesis under mechanical force *in vitro*. Static compressive force-treated hPDLSCs showed a dose-dependent increase in the TRPV4 protein level (Fig. S2). The mRNA levels of IL-6 and TNF-α in hPDLSCs were upregulated after compressive force loading *in vitro* and downregulated by GSK219 (Fig. 5A). Consistently, western blotting results showed that IL-6 and Ki67 protein levels were upregulated after compressive force loading *in vitro* and downregulated by

simultaneous treatment with GSK219 (Fig. 5B and Fig. S3). These findings confirm the effects of the application of static compressive force *in vitro* and the TRPV4 inhibitor GSK219 on hPDLSCs.

The ratio of receptor activator of NF-κB ligand/osteoprotegerin (RANKL/OPG), which is essential for osteoclast differentiation, was next assessed by western blotting. Force application *in vitro* upregulated the RANKL protein level in hPDLSCs, which was reversed by simultaneous treatment with GSK219. By contrast, no significant change in the OPG level was detected. Therefore, the RANKL/OPG ratio increased after compression force application, but this effect was partially blocked by simultaneous treatment with GSK219 (Fig. 5C).

The signaling pathway by which TRPV4 in hPDLSCs regulated osteoclast generation was next investigated. ERK protein kinases can be activated by TRPV4 signaling. Additionally, ERK is involved in the transcriptional regulation of RANKL/OPG [25, 26]. Therefore, we hypothesized that mechanical force-induced upregulation of TRPV4 in hPDLSCs would increase the RANKL/OPG ratio by activating the ERK signaling pathway. To this end, hPDLSCs were pretreated with a small molecule agonist or antagonist of TRPV4 before applying compressive force *in vitro*. Western blotting results showed that the compressive force caused rapid phosphorylation of ERK in hPDLSCs, which was partially attenuated by the additional administration of TRPV4 inhibitor with GSK219 (Fig. 5D). Furthermore, addition of the TRPV4 agonist, GSK101 (10 nM), to hPDLSCs enhanced robust induction of ERK phosphorylation after mechanical force stimulation (Fig. 5E). These results suggest that force-induced TRPV4 in hPDLSCs regulates osteoclast differentiation by affecting the RANKL/OPG system via ERK signaling.

# Discussion

Mechanical force plays an important role in tissue development and homeostasis by modulating stem cell fate [4]. As the main MSCs in the PDL, PDLSCs play an important role in maintaining periodontal tissue homeostasis and alveolar bone remodeling [8–10]. They are mechanosensitive and respond to mechanical stimulation both *in vivo* and *in vitro* [27–29]. PDLSCs mediate the inflammatory process and promote osteoclastogenesis under mechanical stimulation *in vivo*. *In vitro*, mechanical loading—including tension, compression, and vibration—induces PDLSCs to express high levels of proinflammatory cytokines, chemokines, β-2 adrenergic receptor, and $H_2S$ [11–13, 30]. However, the changes in the MSC characteristics of PDLSCs after the mechanical stimulus *in vivo* were unclear. Our study demonstrated that mechanical force application *in vivo* induced PDLSC proliferation, which was associated with inflammatory cytokine accumulation and osteoclast differentiation. Also, mechanical force altered the MSC characteristics of rat primary force-induced PDLSCs isolated *ex vivo* in terms of promoting their proliferation, proinflammatory cytokine secretion, and immunoregulation of macrophage migration and osteoclast differentiation, but suppressed their differentiation ability. These results indicate the changes in the MSC characteristics of PDLSCs induced by mechanical force *in vivo*.

MSCs are sensitive to mechanical force. Various mechanosensors have been proposed to be involved in modulating MSC differentiation under mechanical stimuli *in vitro*, including the mobilization of second

messengers, ion channels, the cytoskeleton, primary cilia, membrane proteins such as integrins, or through changes in cellular structure [14, 15]. However, the mechanotransduction mechanism of PDLSCs, the main MSCs in the mechanical sensor of periodontal tissues, is unclear. $Ca^{2+}$ influx in PDLSCs has been reported following mechanical stimuli [19]. Previous studies have shown that the level of cytoskeletal remodeling influenced the mechanically driven osteogenic differentiation of PDLSCs [32]. A piezo channel has also been proven to sense mechanical signals and regulate stem cell behaviors [33]; however, it is reportedly not associated with ultrasound-related signal-stimulated PDLSC proliferation [34]. In this study, the expression of TRPV4, a calcium channel, was increased in PDLSCs under mechanical force *in vivo*. This suggests that TRPV4 plays an important role in the transduction of mechanical stimuli in PDLSCs and may mediate subsequent biological responses.

TRPV4 is a calcium channel involved in the sensation of different stimuli in various cells and tissues [16, 17, 35]. TRPV4 activation is associated with the inflammatory response and promotes proinflammatory cytokine release by various types of tissues and cells. Moreover, mutations in TRPV4 are linked to inherited disorders of bone metabolism [16]. MSCs isolated from TRPV4-knockout mice demonstrated an impaired osteogenic potential [17]. In this study, the expression of TRPV4 was upregulated in PDLSCs under mechanical force *in vivo*. Inhibition of TRPV4 in force-loaded PDLSCs isolated *ex vivo* decreased their proliferation, osteoclastic differentiation, and expression of inflammation-related cytokines. Consistently, TRPV4 activation mediated hPDLSC biological responses to mechanical force, which were reversed by a simultaneous treatment with GSK219. These results indicate that mechanical force increased TRPV4 expression and function, and thereby triggering subsequent behaviors, which can be partially blocked by TRPV4 deactivation. Thereby, TRPV4, as a regulator, mediate the mechanical response in PDLSCs.

PDLSCs modulate alveolar bone remodeling under mechanical stimuli by inducing bone formation on the tension side and bone resorption on the compression side of periodontal tissues [36]. Zhang and colleagues found that compressive force activated the Wnt/β-catenin pathway in human PDLSCs [37]. Our previous studies showed that PDLSCs highly express β-2 adrenergic receptor and produce a high level of $H_2S$ under a static compression stimulus to increase the RANKL/OPG ratio and promote osteoclastic differentiation [19, 27]. In addition, PDLSCs induce polarization of inflammatory M1 macrophages, thereby contributing to osteoclastogenesis. In this study, the ERK protein kinase signaling pathway, which is essential for osteoclastogenesis, was evaluated [38, 39]. The static compressive force induced the phosphorylation of ERK in PDLSCs, which was partially rescued by treatment with the TRPV4 inhibitor GSK219. The same trend in the RANKL/OPG ratio was detected. These data suggest that mechanical force-induced TRPV4 activation in PDLSCs promotes osteoclastogenesis via the phosphorylation of ERK protein kinases.

# Conclusion

In summary, we show here that the activation of TRPV4 in PDLSCs under mechanical force contributes to the changes in their biological properties including clonogenicity, proliferation, multipotent differentiation,

and immunoregulation and modulates bone remodeling during tooth movement (Fig. 6). These results suggest a critical role for PDLSCs in mechanical force-induced bone remodeling and indicate the importance of TRPV4 in regulating PDLSC function and mediating bone remodeling under mechanical force. The findings also imply that targeting TRPV4 might benefit mechanical force-induced bone remodeling and tooth movement.

## Abbreviations

PDLSCs: Periodontal ligament stem cells; MSCs: Mesenchymal stem cells; PDL: Periodontal ligament; TRP: Transient receptor potential; TRPV4: TRP subfamily V member 4; TRAP: Tartrate-resistant acid phosphatase; CFU-F: Colony forming units-fibroblastic; TNF-α: Tumor necrosis factor-α; MCP-1: Monocyte chemoattractant protein -1; RANKL: Nuclear factor-κB ligand; OPG: osteoprotegerin.

## Declarations

# Ethics approval and consent to participate

The animal experimental protocols were approved by the Institutional Animal Care and Use Committee of Peking University (LA2013-92). Permission to obtain extracted teeth for human PDLSCs was provided by the Ethics Committee of Peking University (PKUSSIRB-201311103).

# Consent for publication

Not applicable.

# Availability of data and materials

The datasets used and/or analyzed during the current study are available from the corresponding author on reasonable request.

# Competing interests

The authors declare that they have no competing interests.

# Funding

This work was supported by the Projects of Ten-Thousand Talents Program (Y.L.), Beijing Municipal Natural Science Foundation No. L182005 (Y.L), and National Natural Science Foundations of China No. 81871492 (Y.L.), No.81600893 (D.H.) and No. 81801031 (H.Y.).

# Authors' contributions

S.J. and D.H. performed the experiments, collected and analyzed the data, and wrote the manuscript. Y.W., T.Z., H.Y., and Y.Z. contributed to collection and assembly of data. X.L. and L.Z. performed the experiments. D.H. and Y.L. contributed to overall design of the study, critically editing the manuscript. All authors reviewed and approved the manuscript.

# Acknowledgements

The authors acknowledge the financial support from the Projects of Ten-Thousand Talents Program (Y.L.), Beijing Municipal Natural Science Foundation No. L182005 (Y.L), and National Natural Science Foundations of China No. 81871492 (Y.L.), No.81600893 (D.H.) and No. 81801031 (H.Y.).

# References

1. Zhang L, Issa BS, Chen T, Zhou B, Xu Q. Role of Resident Stem Cells in Vessel Formation and Arteriosclerosis. Circ Res. 2018;122:1608-24.
2. Shi YF, Wang Y, Li Q, Liu K, Hou J, Shao C, Wang Y. Immunoregulatory mechanisms of mesenchymal stem and stromal cells in inflammatory diseases. Nat Rev Nephrol. 2018;14:493-507.
3. Volponi AA, Pang Y, Sharpe PT. Stem cell-based biological tooth repair and regeneration. Trends Cell Biol. 2010;20:715-22.
4. Vining K, Mooney D. Mechanical forces direct stem cell behaviour in development and regeneration. Nat Rev Mol Cell Biol. 2017;18:728-42.
5. Liaw NY, Zimmermann WH. Mechanical stimulation in the engineering of heart muscle. Adv Drug Deliv Rev. 2016;96:156-60.
6. Papachroni KK, Karatzas DN, Papavassiliou KA, Basdra EK, Papavassiliou AG. Mechanotransduction in osteoblast regulation and bone disease. Trends Mol Med. 2009;15:208-16.
7. Le HQ, Ghatak S, Yeung CY, Tellkamp F, Günschmann C, Dieterich C, et al. Mechanical regulation of transcription controls Polycomb-mediated gene silencing during lineage commitment. Nat Cell Biol. 2016;18: 864-75.
8. Kinane DF, Stathopoulou PG, Papapanou PN. Periodontal diseases. Nat Rev Dis Primers. 2017;3:17038.
9. Meikle MC. The tissue, cellular, and molecular regulation of orthodontic tooth movement: 100 years after Carl Sandstedt. Eur J Orthod. 2006;28:221-40.
10. Seo BM, Miura M, Gronthos S, Bartold PM, Batouli S, Brahim J, et al. Investigation of multipotent postnatal stem cells from human periodontal ligament. Lancet. 2004;364:149-55.
11. He DQ, Kou XX, Yang RL, Liu DW, Wang XD, Luo Q, et al. M1-like Macrophage Polarization Promotes Orthodontic Tooth Movement. J Dent Res. 2015;94:1286-94.

12. Liu FF, Wen FJ, He DQ, Liu DW, Yang R, Wang X, et al. Force-Induced H2S by PDLSCs Modifies Osteoclastic Activity during Tooth Movement. J Dent Res. 2017;96:694-702.
13. Wang Y, Li Q, Liu FF, Jin SS, Zhang YM, Zhang T, et al. Transcriptional activation of glucose transporter 1 in orthodontic tooth movement-associated mechanical response. Int J Oral Sci. 2018;4:244-52.
14. Douguet D, Honoré E. Mammalian Mechanoelectrical Transduction: Structure and Function of Force-Gated Ion Channels. Cell. 2019;179:340-54.
15. Nilius B, Owsianik G. The transient receptor potential family of ion channels. Genome Biol. 2011;12:218.
16. Kang SS, Shin SH, Auh C K, Chun J. Human skeletal dysplasia caused by a constitutive activated transient receptor potential vanilloid 4 (TRPV4) cation channel mutation. Exp Mol Med. 2012; 44:707-22.
17. O'Conor, CJ, Griffin TM, Liedtke W, Guilak F. Increased susceptibility of Trpv4-deficient mice to obesity and obesity-induced osteoarthritis with very high-fat diet. Ann Rheum Dis. 2012;72:300-04.
18. Dunn MD, Park CH, Kostenuik PJ, Kapila S, Giannobile WV. Local delivery of osteoprotegerin inhibits mechanically mediated bone modeling in orthodontic tooth movement. Bone. 2007; 41:446-55.
19. Cao HF, Kou XX, Yang RL, Liu DW, Wang XD, Song Y, et al. Force-induced Adrb2 in periodontal ligament cells promotes tooth movement. J Dent Res. 2014; 93:1163-69.
20. Parfitt AM, Drezner MK, Glorieux FH, Kanis JA, Malluche H, Meunier PJ, et al. Bone histomorphometry: standardization of nomenclature, symbols, and units. Report of the ASBMR Histomorphometry Nomenclature Committee. J Bone Miner Res. 1987;2:595-610.
21. Kou XX, Wu YW, Ding Y, Hao T, Bi RY, Gan YH, et al. 17 beta-estradiol aggravates temporomandibular joint inflammation through the NF-kappab pathway in ovariectomized rats. Arthritis Rheum. 2011; 63:1888-97.
22. Saito A , Nagaishi K, Iba K, Mizue Y, Chikenji T, Otani M, et al. Umbilical cord extracts improve osteoporotic abnormalities of bone marrow-derived mesenchymal stem cells and promote their therapeutic effects on ovariectomised rats. Sci Rep. 2018;8:1161.
23. Ye L, Kleiner S, Wu J, Sah R, Gupta RK, Banks AS, et al. TRPV4 Is a Regulator of Adipose Oxidative Metabolism, Inflammation, and Energy Homeostasis. Cell. 2012;151:96-110.
24. Klein AH, Trannyguen M, Joe CL, Iodi CM, Carstens E. Thermosensitive transient receptor potential (TRP) channel agonists and their role in mechanical, thermal and nociceptive sensations as assessed using animal models. Chemosens Percept. 2015;8:96-108.
25. Ang E, Liu Q, Qi M, Liu HG, Yang X, Chen H, et al. Mangiferin attenuates osteoclastogenesis, bone resorption, and RANKL-induced activation of NF-κB and ERK. J Cell Biochem. 2011;112:89-97.
26. Miyazaki T, Katagiri H, Kanegae Y, Takayanagi H, Sawada Y, Yamamoto A, et al. Reciprocal Role of ERK and Nf-κb Pathways in Survival and Activation of Osteoclasts. J Cell Biol. 2000;148:333-42.

27. Feng L, Yang R, Liu D, Wang X, Song Y, Cao H, et al. PDL Progenitor-Mediated PDL Recovery Contributes to Orthodontic Relapse. J Dent Res. 2016;95:1049-56.
28. Shen T, Qiu L, Chang H, Yang Y, Jian C, Xiong J, et al. Cyclic tension promotes osteogenic differentiation in human periodontal ligament stem cells. Int J Clin Exp Pathol. 2014; 7:7872-80.
29. Mussig E, Schulz S, Spatz J P, Ziegler N, Tomakidi P, Steinberg T. Soft micropillar interfaces of distinct biomechanics govern behaviour of periodontal cells. Eur J Cell Biol. 2010;89:315-25.
30. Lee SI, Park KH, Kim SJ, Kang YG, Lee YM, Kim EC. Mechanical stress-activated immune response genes via Sirtuin 1 expression in human periodontal ligament cells. Clin Exp Immunol. 2012;168:113-24.
31. Zhang CX, Lu YQ, Zhang LK, Liu Y, Zhou Y, Chen Y, et al. Influence of different intensities of vibration on proliferation and differentiation of human periodontal ligament stem cells. Arch Med Sci. 2015, 11:638-46.
32. Mcbeath R, Pirone DM, Nelson CM, Bhadriraju K, Chen CS. Cell Shape, Cytoskeletal Tension, and RhoA Regulate Stem Cell Lineage Commitment. Dev Cell. 2004;6:483-95.
33. He L, Si G, Huang J, Samuel ADT, Perrimon N. Mechanical regulation of stem-cell differentiation by the stretch-activated Piezo channel. Nature. 2018;555:103-06.
34. Gao Q, Cooper PR, Walmsley AD, Scheven BA. Role of Piezo Channels in Ultrasound-stimulated Dental Stem Cells. J Endod. 2017;43:1130-36.
35. Rock MJ, Prenen J, Funari VA, Funari TL, Merriman B, Nelson SF, et al. Gain-of-function mutations in TRPV4 cause autosomal dominant brachyolmia. Nat Genet. 2008;40:999-1003.
36. Garlet TP, Coelho U, Silva JS, Garlet GP. Cytokine expression pattern in compression and tension sides of the periodontal ligament during orthodontic tooth movement in humans. Eur J Oral Sci. 2007;115:355-62.
37. Zhang L, Liu W, Zhao J, Ma X, Shen L, Zhang Y, et al. Mechanical stress regulates osteogenic differentiation and RANKL/OPG ratio in periodontal ligament stem cells by the Wnt/β-catenin pathway. Biochim Biophys Acta. 2016;1860:2211-19.
38. Giulia CG, Mehdi D, Mickael R, Vinod M, Louvet L, Copin C, et al. Human Alternative Macrophages Populate Calcified Areas of Atherosclerotic Lesions and Display Impaired RANKL-Induced Osteoclastic Bone Resorption Activity. Circ Res. 2017;121:19-30.
39. Wang LJ, Iorio C, Yan K, Yang H, Takeshita S, Kang S, et al. A ERK/RSK-mediated negative feedback loop regulates M-CSF–evoked PI3K/AKT activation in macrophages. FASEB J. 2018; 32: 875–87.

# Figures

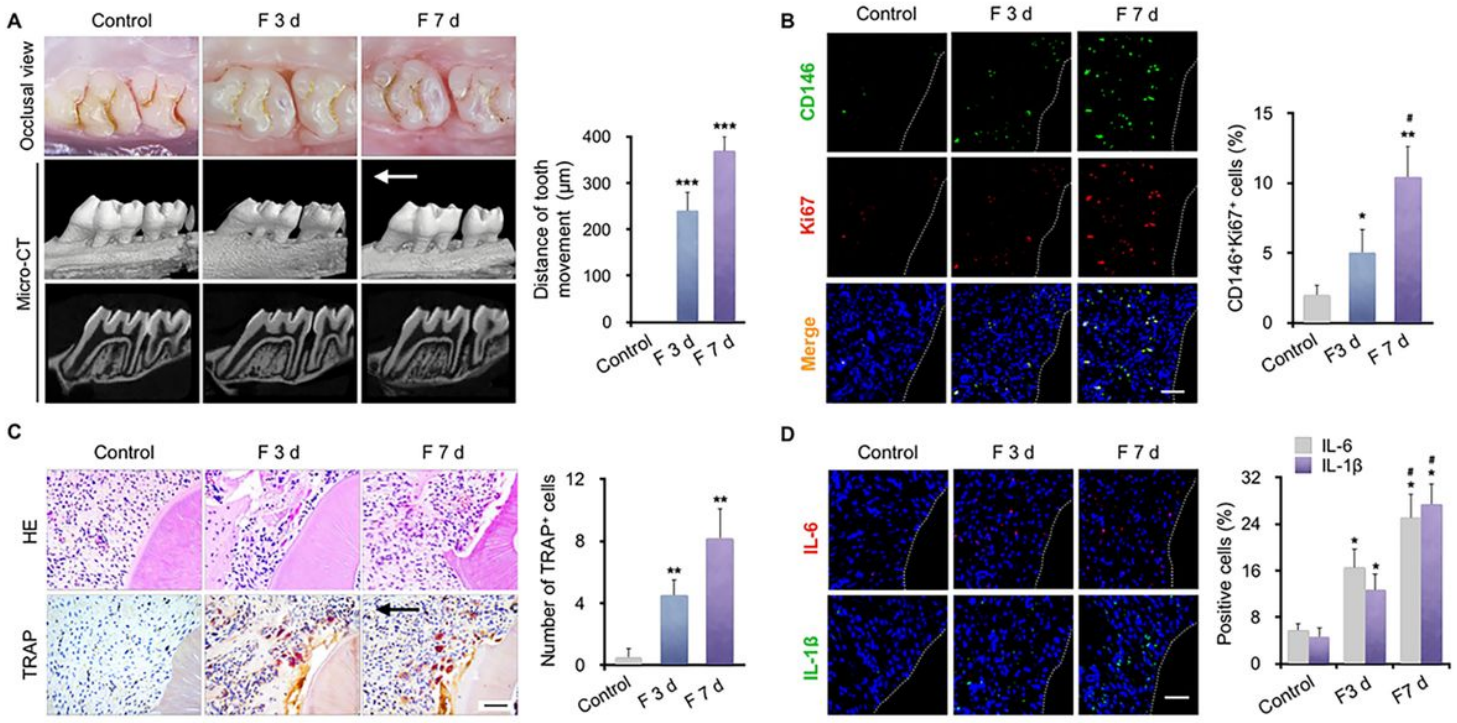


## Figure 1

PDLSCs and osteoclasts accumulate on the compression side of periodontal tissues following application of mechanical force in vivo. (A) Representative occlusal view and micro-CT images of tooth movement for 3 and 7 days. Semi-quantitative analysis showed that the distance of tooth movement gradually increased after force was applied for 3 and 7 days (F 3 d and F 7 d, n = 6). The arrow shows the direction of mechanical force. ***P < 0.001 versus control. (B) Representative immunofluorescence images of the compression side of distobuccal roots. The number of CD146+ (green) and Ki67+ (red) PDLSCs was increased in F 3 d and F 7 d. N = 6, *P < 0.05, **P < 0.01, versus control, #P < 0.05 versus F 3 d. Scale bar: 100 μm. (C) Representative H&E and TRAP staining of the compression side of distobuccal roots. The number of TRAP-positive osteoclasts was increased in the periodontal tissues after force application. The arrow shows the direction of mechanical force. Scale bar: 100 μm. N = 6, **P < 0.01 versus control. (D) Representative immunofluorescence staining and semi-quantitative analysis of IL-6 and IL-1β in the periodontal tissues after force was applied. The number of cells positive for IL-6 and IL-1β increased around the periodontal tissues after force was applied. Scale bar: 100 μm. N = 6, *P < 0.05 versus control. #P < 0.05 versus F 3 d.

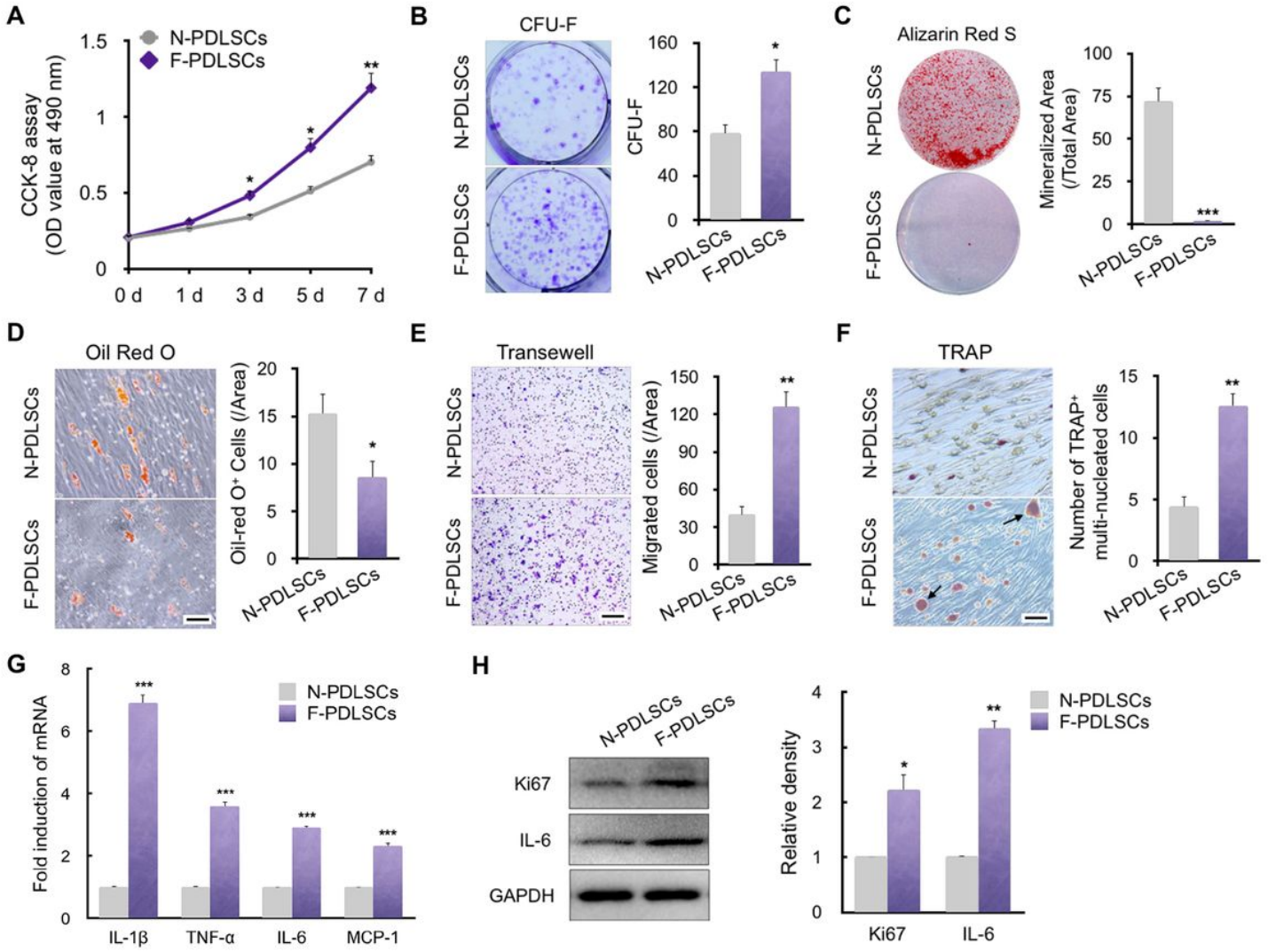


## Figure 2

Biological characteristics of force-induced rPDLSCs ex vivo. (A) Growth curves of force-induced PDLSCs (F-PDLSCs) and normal PDLSCs (N-PDLSCs) as determined by CCK-8 assay. F-PDLSCs and N-PDLSCs isolated ex vivo proliferated at a similar rate for 1–2 days, but F-PDLSCs showed faster proliferation after 3 days. N = 6, *P < 0.05, **P < 0.01 versus N-PDLSCs. (B) Representative images and quantitative comparison of colony-forming units fibroblastic (CFU-F) of two different rPDLSCs. N = 6, *P < 0.05 versus N-PDLSCs. (C) Compared to N-PDLSCs, the F-PDLSCs showed a decreased capacity to form mineralized nodules, assessed by ARS staining and quantification. N = 5, ***P < 0.001 versus N-PDLSCs. (D) Oil Red O staining and quantification of two different rPDLSCs. F-PDLSCs showed less accumulation of lipid-rich vacuoles. N = 5, *P < 0.05 versus N-PDLSCs. Scale bar: 400 μm. (E) Representative images of crystal violet staining of RAW264.7 macrophages in Transwell assays. Conditional medium from F-PDLSCs enhanced the migration of macrophages compared with the control. N = 6, **P < 0.01 versus N-PDLSCs. Scale bar: 400 μm. (F) Representative images of TRAP staining of osteoclasts among RAW264.7 macrophages co-cultured with PDLSCs. Osteoclastic differentiation of RAW264.7 macrophages was significantly enhanced by force loading. N = 6, **P < 0.01 versus N-PDLSCs. Scale bar: 200 μm. (G)

Relative mRNA levels of inflammation-related genes. The mRNA levels of IL-1β, TNF-α, IL-6, and MCP-1 were upregulated in the F-PDLSCs group. ***P < 0.001 versus N-PDLSCs. (H) Western blot of Ki67 and IL-6. The protein levels of Ki67 and IL-6 were upregulated in the force-treated PDLSCs group. *P < 0.05, **P < 0.01 versus N-PDLSCs. Three independent assays were performed for each cell population.

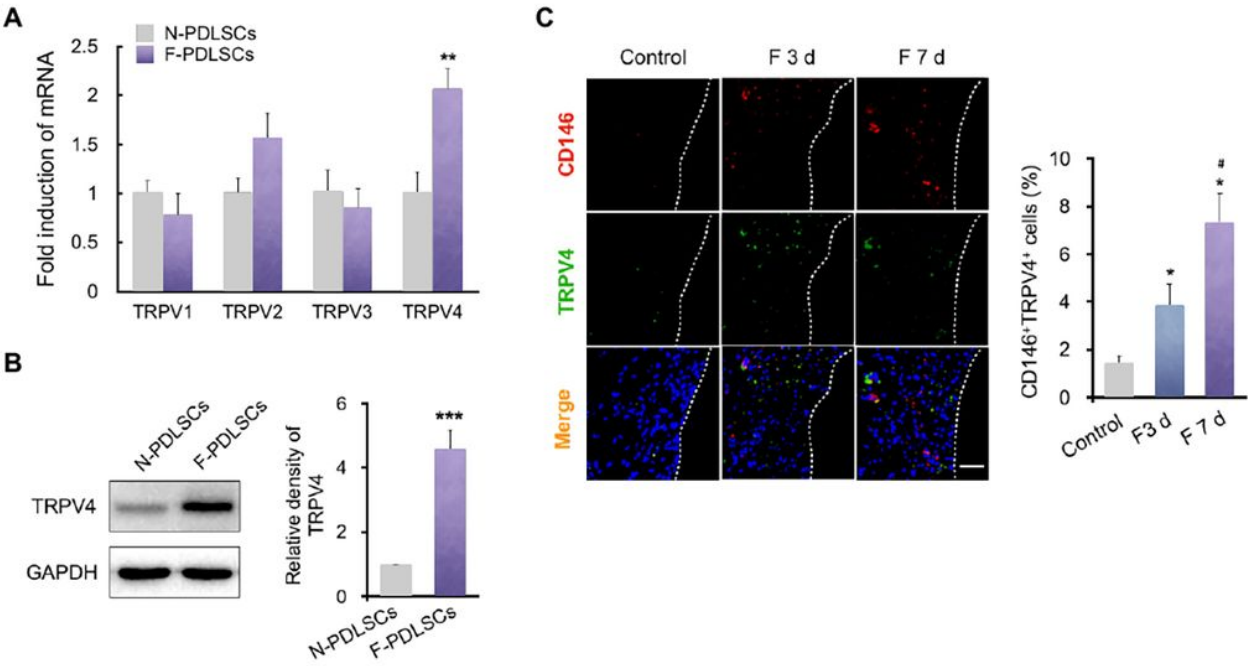


## Figure 3

TRPV4 was present in F-PDLSCs ex vivo. (A) Relative mRNA levels of TRPV1–4. TRPV1–4 mRNAs were detected in rPDLSCs, while that of TRPV4 was increased in the F-PDLSCs. **P < 0.01 versus N-PDLSCs. (B) Western blot of TRPV4 in rPDLSCs. The TRPV4 protein level in rPDLSCs was upregulated after force loading. ***P < 0.001 versus N-PDLSCs. (C) Representative immunofluorescence images and semi-quantitative analysis of the compression side of distobuccal roots. The number of CD146+ (red) and TRPV4+ (green) PDLSCs was increased in F 3 d and F 7 d. N = 6, *P < 0.05 versus control, #P < 0.05 versus F 3 d. Scale bar: 100 μm. Data are means ± SD of three independent experiments.

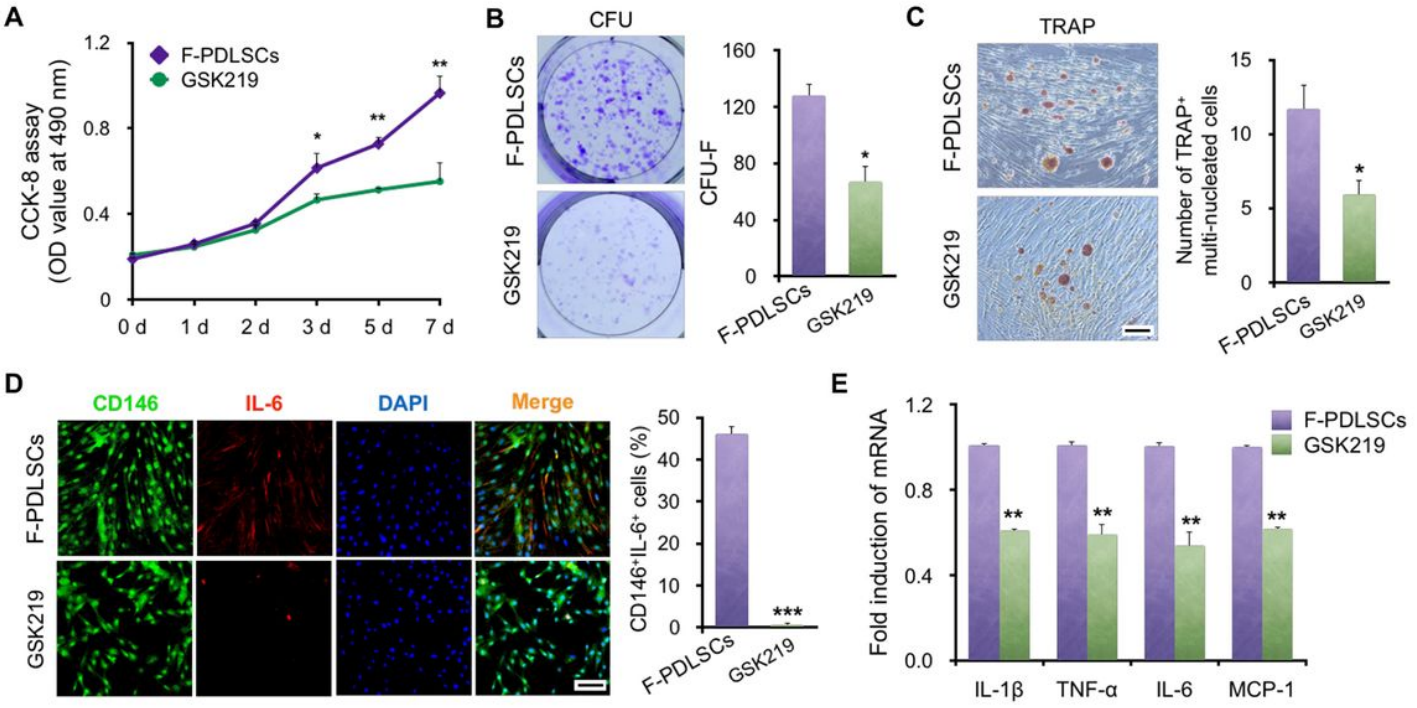


## Figure 4

Inhibition of TRPV4 represses biological characteristics of F-PDLSCs ex vivo. (A) Growth curves of F-PDLSCs and GSK219-pretreated PDLSCs (GSK219). CCK-8 assays showed that the promotion of proliferation after force loading was inhibited by the TRPV4 antagonist GSK219. N = 6, *P < 0.05, **P < 0.01 versus F-PDLSCs. (B) Representative images and quantitative comparison of CFU-F of two different rPDLSCs. N = 6, *P < 0.05 versus F-PDLSCs. (C) Representative images of TRAP staining of osteoclasts among RAW264.7 macrophages co-cultured with rPDLSCs. TRAP staining showed a significant decline in the number of TRAP+ osteoclasts among GSK219-pretreated PDLSCs. N = 6, *P < 0.05 versus F-PDLSCs. Scale bar: 200 μm. (D) Representative immunofluorescence images of F-PDLSCs and GSK219-pretreated PDLSCs. The number of CD146 (green) and IL-6 (red) double-stained PDLSCs decreased after GSK219 treatment. N = 5, ***P < 0.001 versus F-PDLSCs. Scale bar: 50 μm. (E) Relative mRNA levels of inflammation-related genes. The mRNA levels of IL-1β, TNF-α, IL-6, and MCP-1 were decreased in GSK219-pretreated PDLSCs. Three independent assays were performed for each cell population.

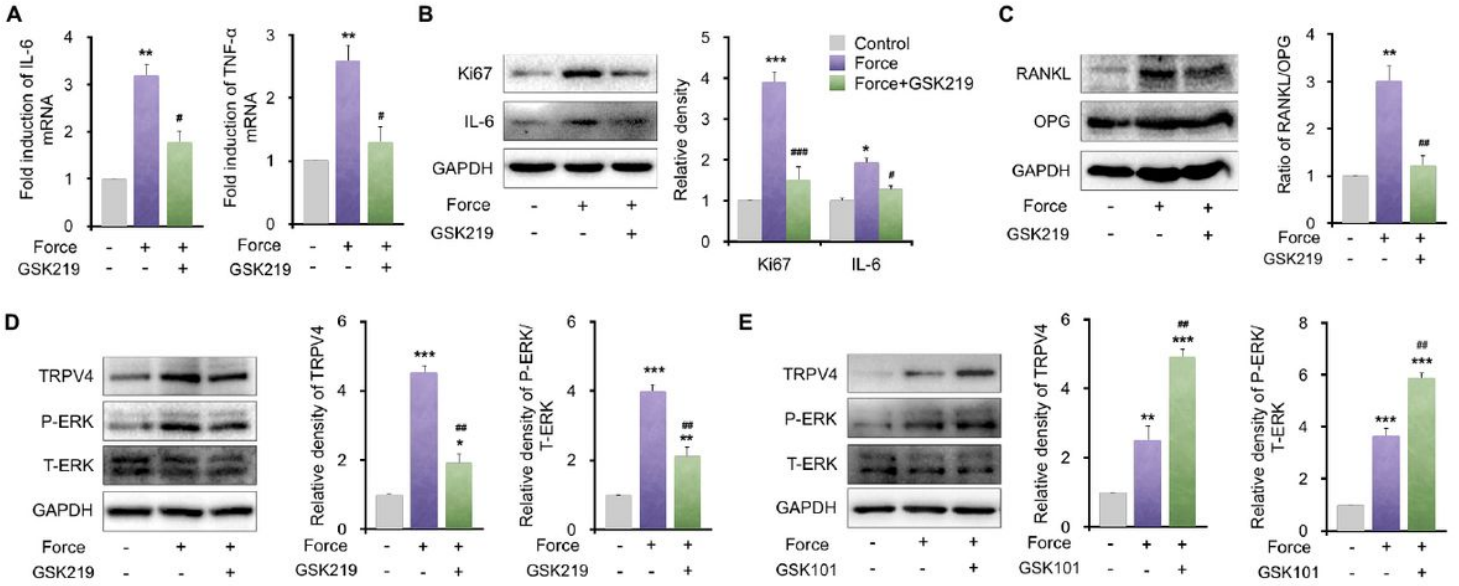


## Figure 5

TRPV4 regulated force-induced inflammation-related gene expression and the receptor activator of nuclear factor-κB ligand (RANKL)/osteoprotegerin (OPG) system in hPDLSCs via the ERK signaling pathway. (A) Relative mRNA levels of inflammation-related genes. The mRNA levels of IL-6 and TNF-α were upregulated in the force group and downregulated in the force + GSK219 group compared with the force group. (B) Western blot and semi-quantifications of Ki67 and IL-6 in hPDLSCs. The protein levels of Ki67 and IL-6 were upregulated after mechanical force loading, which was mostly reversed by TRPV4 treatment. GAPDH served as an internal control for equal loading. (C) GSK219 inhibition of TRPV4 decreased the force-induced upregulation of the RANKL/OPG ratio. The protein levels of RANKL and OPG were determined in control PDLSCs or cells subjected to mechanical force with or without GSK219 treatment. (D) Western blot and semi-quantifications of TRPV4, phosphorylated ERK (P-ERK), and total ERK (T-ERK) levels in hPDLSCs. The TRPV4 level and the proportion of P-ERK/T-ERK were upregulated after mechanical force application and attenuated by the inhibition of TRPV4. (E) Western blot and semi-quantifications of TRPV4, phosphorylated ERK (P-ERK), and total ERK (T-ERK) levels in hPDLSCs. The TRPV4 level and the proportion of P-ERK/T-ERK were upregulated after mechanical force stimulation and further enhanced by a simultaneous treatment with GSK101. Data are means ± SD of three independent experiments. *P < 0.05, **P < 0.01, ***P < 0.001 versus control. #P < 0.05, ##P < 0.01, ###P < 0.001 versus force.

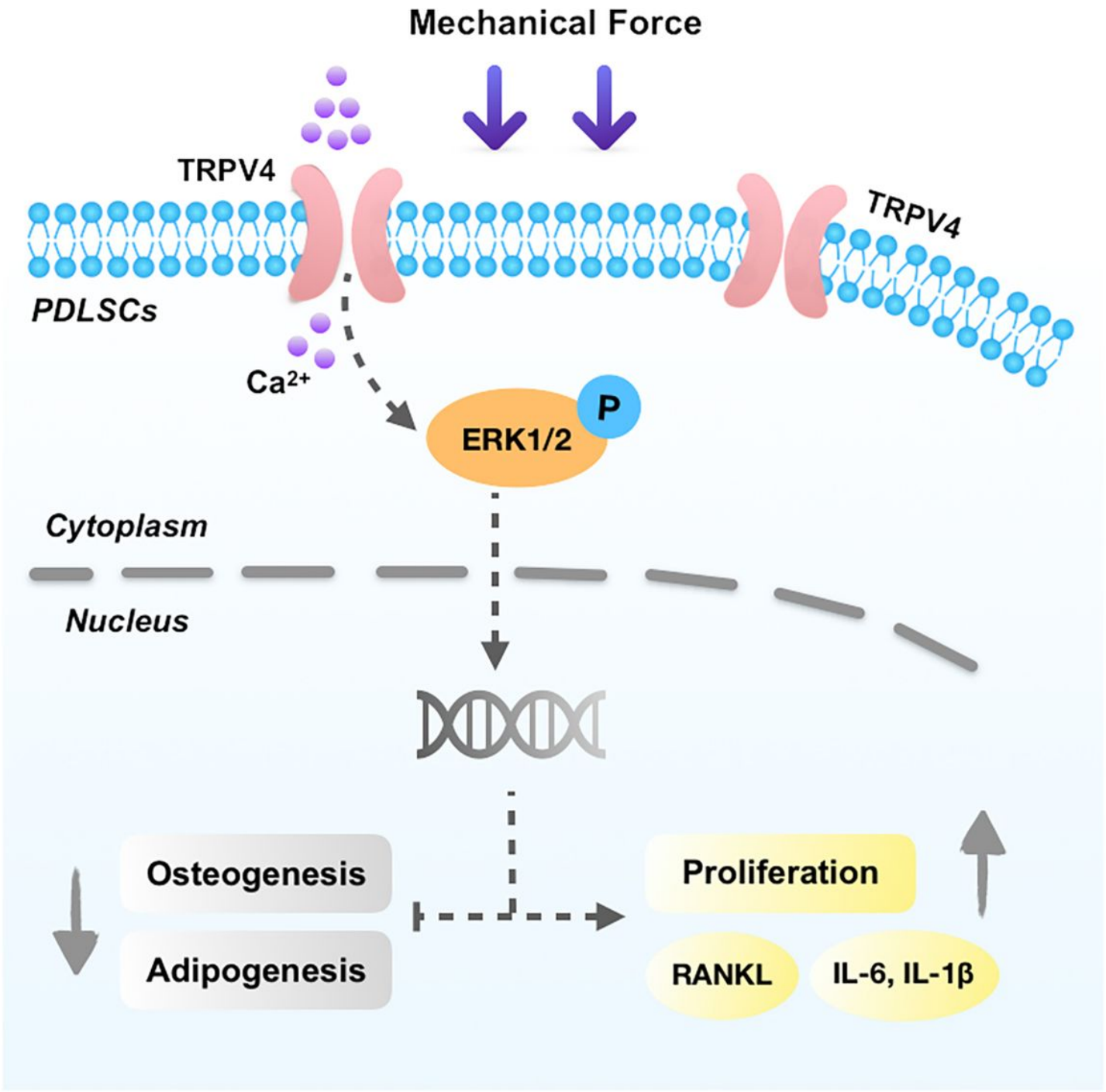


**Figure 6**

The activation of TRPV4 in PDLSCs under mechanical force contributes to the changes in their biological properties and modulates bone remodeling during tooth movement.

## Supplementary Files

This is a list of supplementary files associated with this preprint. Click to download.

- SupportingInformation.docx